



Internship report for the fulfillment of the Master of Science Degree: « Optique : de la Science à la Technologie » of the Institut d'Optique Graduate School.

Non Blinking CdSe/CdS Core-Shell Quantum Dots Observed with Fluorescence Lifetime Microscopy

The internship is fulfilled from March 8 to July 9, 2010 under the direction of Benoit Dubertret from the « Physique et Etude des Matériaux » Group at the Ecole Supérieure de Physique et de Chimie Industrielles de la Ville de Paris – ParisTech.

This report is submitted on June 17, 2010. The oral presentation will be held on June 24, 2010.

Author: Arjen Dijksman



Table of contents

Table of contents	2
Acknowledgments	3
Introduction	4
The physics of fluorescent semiconductor nanocrystals	6
Core-Shell CdSe-CdS Quantum Dots	8
Chemical synthesis of the quantum dots	12
General principles	12
Investigated quantum dots.....	12
Fluorescence Lifetime Scanning Microscopy	13
Principles of Fluorescence Lifetime Scanning Microscopy.....	13
MicroTime 200 experimental setup	14
Overview	14
Laser excitation	15
Confocal unit with Olympus IX71 microscope.....	15
Single Photon Detectors.....	16
Acquisition card and software.....	16
Cryostat	16
Spectroscope.....	16
Practical operation.....	16
Measurement results.....	18
Preliminary results.....	18
Introductory measurements	18
Core shell CdSe/CdS quantum dots (sample 101026)	19
CdSe quantum platelets	22
Measurements series on the PP, PG, GP and GG quantum dots.....	24
Observation of fluorescent QDs with the eye under microscope.....	24
Emission spectra of quantum dots.....	24
Fluorescence lifetime of dots in solution	25
MicroTime 200 results	25
Comparative results at room temperature	25
Results from 4 K to 300 K for GG sample.....	28
Discussion and conclusion	31
Bibliography	32
Glossary.....	34
Appendix	35

Acknowledgments

I would like to thank many people for the fulfillment of this Quantum Dot related Master of Science internship.

First of all, I thank Dr. Benoît Dubertret for accepting me in his research group and placing confidence in a newbie student with an atypical curriculum of physics engineering and master of optics, interrupted by 20 years of project management in a totally different field. Thank you for initiating me in the physics and experimental behavior of those likeable and thought-provoking quantum dots.

I would also like to thank warmly all members of the LPEM research group who welcomed me in a world of chemistry preparations, optical setups, group meetings, physics discussions and lunch and coffee breaks. Research is a human adventure and I am convinced that it can only flourish with the participation of diverse sensibilities. Thanks especially to Clémentine, Benoît M., Mickaël who worked more directly with me on the microscope, or who provided insight in the way how the samples were prepared. Thanks to Pierre, Vincent, Ivan, Eduardo for improvements of the MicroTime experimental setup. Thanks to the other members of the LPEM group for your helpful hand, your advice and good humor!

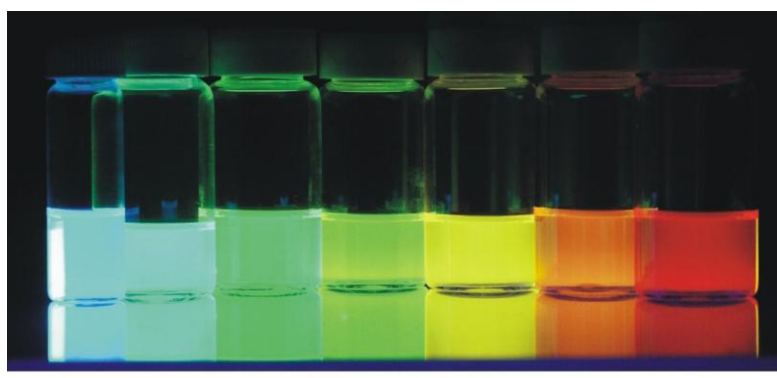
In the framework of my Master of Science, I would also like to thank the Institut d'Optique staff: Nathalie Westbrook who welcomed me in September 2008 with my awkward request to follow some regular Master of Science courses while still engaged with my employer, Nicolas Dubreuil for welcoming me in the Master 2 program and giving the right advice for the next steps. Special thanks also to Véronique Dorn, for all the supporting work of the Master program.

Above all I would like to thank my wife Laurence, without whose help I would never have been able to engage in this new stage of my life.

Thanks also to my ex-SFR colleague Salwa Ansart, for interesting physics and mathematics discussions, and to my previous employer SFR who provided the financial support for this year.

Introduction

During the 1980s, it was discovered that tiny semiconductor crystals whose size is a few millionths of a millimeter (so called nanocrystals) revealed behaviour that was in a way analogous to the behaviour of single atoms and molecules [1, 2]. Under illumination, the colour of the absorbed and emitted light depends on the size of the nanocrystal, while their composition remains the same (see Figure 1). With respect to bulk semiconductors, the strong confinement of the electrons in the nanocrystal induces a transition to a quantum regime. They behave like quantum particles, hence their surname Quantum Dots (abridged QDs). It was realized that one could shape “artificial” atoms in this way, with emission and absorption properties at wish. This promising perspective brought forth a wealth of experimental and theoretical work on QDs, aiming at better controlling their size and shape, at facilitating their manipulation and at directing their optical and electronic behaviour.



2.3 → 5.5
Size (nanometers)

© Copyright 2004, Benoit Dubertret

Figure 1: Colloidal solutions of quantum dots of increasing size.

The LPEM group of Benoît Dubertret in which I carried out my internship is specialized in the chemical synthesis and the optical characterization of quantum dots in colloidal solutions. As a matter of fact, due to their chemical expertise, the people of this group are forerunners in the race towards the perfect quantum dot: they were first at preparing non-blinking, 100% efficient quantum dots [3]. What this exactly means will be presented in this report. I had indeed the opportunity to run single quantum dot - single photon time resolved measurements on exceptionally efficient and stable core-shell Cadmium Selenide / Cadmium Sulphide quantum dots (CdSe/CdS), the first of that type. As the LPEM group acquired a new Fluorescence Lifetime Microscope (so called MicroTime 200), I had the privilege to initiate measurements on that setup.

After a presentation of the history and the theory of quantum dots and their fluorescence, as well as the way colloidal solutions of QDs are prepared, I will present the specificities of the MicroTime200 and the way it was used to characterize the CdSe/CdS quantum dots, as well as their present and nice-to-have add-ons, which greatly facilitate the investigation of the QDs. After a series of introductory measurements on ad hoc samples prepared in the laboratory, four types of core-shell QDs have been (and are presently still) systematically investigated. The measurement results are exposed with some discussion, the main point

being the observation of exceptionally stable large core / thick shell CdSe/CdS fluorescence time traces. I will conclude with some open perspectives for future study.

The physics of fluorescent semiconductor nanocrystals

One should not work on semiconductors, it is a filthy mess; who knows if semiconductors exist after all.

Wolfgang Pauli [4]

Research on the fluorescence of semiconductor nanocrystals is at the crossroads of different scientific fields. Firstly, **fluorescence** relates to emitted light and therefore to optics and photonics. Secondly, **semiconductors** involve electronic bandgaps, electron-hole physics and electronics. Thirdly, **nanocrystals** pertain to nanotechnology which takes advantage of the peculiar rules of quantum physics. Fourth, **colloids** imply chemistry and refined preparation techniques. All with all it is a multidisciplinary and rewarding research field.

The distinctive feature of **semiconductors** has been discovered in the 1830s. Michael Faraday noticed that the conductivity of silver sulphide improved with increasing temperature, while normal conductors become less conductive when they are heated [5]. Alexandre-Edmond Becquerel discovered that shining sunlight on a silver chloride coated electrode increased its conductivity [6]. But it was not until the advent of quantum mechanics that one could devise a successful theory for the conductivity of semiconductors. Two days after Pauli's desperate statement about semiconductors in a letter to Rudolf Peierls [4], the Royal Society published a paper by Alan Herries Wilson, which explained that for semiconductors, energy must be supplied to the outer bound atomic electrons – the valence electrons – in order to be raised above a forbidden gap and being allowed to circulate through its crystalline structure under the influence of a voltage [7]. Faraday supplied thermal energy, Becquerel supplied electromagnetic radiation energy but any form of energy would do. One could for example also raise the energy of the valence electrons by doping the crystalline structure with impurity atoms. Or one could supply mechanical energy by way of pressure, inducing piezoconductivity.

Once electrons are raised above the bandgap energy, they can circulate through the crystal, while leaving holes of positive charge at the locations they left. These holes play an important role in the electron dynamics of the semiconductor. The holes can migrate and attract the conduction electrons, giving Coulomb interacting electron-hole pairs, so called excitons. There is a finite probability that an electron and a hole recombine, paying back the energy they lose. This energy payback can be substantiated by radiative (**fluorescence** photons) or non-radiative (phonons, Auger or electron-electron scattering) decay. The nature of the fluorescent light depends on the physical environment of the electron-hole pair just before it recombined. Strong confinement of the exciton in a **nanocrystal** yields quantum-mechanical effects with discretization of the fluorescence peaks. These effects were first discovered in semiconductor nanocrystals by A. Ekimov in a glass matrix [1] and by L. Brus in colloidal solutions [2]. Promising applications for biocellular-tracking, photovoltaics, nanoelectronics and quantum computing attracted much interest towards the semiconductor nanocrystals, which where coined by the popular term Quantum Dots. The different competing groups are mainly organized by the way these quantum dots are prepared. At ESPCI, the QDs are prepared by chemical synthesis and stabilized in **colloidal solutions**. Other possibilities are to grow quantum dots by way of molecular beam or vapour deposition growth on a crystalline substract.

We saw that the colour of the fluorescent light emitted by the quantum dot depended on the electronic confinement. In quantum mechanics, changes that affect light are always induced by changes induced to electrons. It is therefore important to understand the behaviour of the electrons and the photons during the fluorescence. As a matter of fact, fluorescence is the property of a material to emit light of a specific colour after being illuminated by light of a more energetic colour, while the electrons return in their original state. This specific colour emission distinguishes fluorescence from ordinary reflection or diffraction (re-emitting light of the same colour as the illumination) or scattering (re-emitting light with a colour slightly shifted with respect to illumination colour). The delay after which the light is emitted distinguishes fluorescence from luminescence (shorter delays, less than 10 ps) and phosphorescence (longer delays, more than 1 μ s). Investigation of the fluorescence of crystalline semiconductors has a long history because it was discovered experimentally as soon as 1866 by Théodore Sidot, when he prepared colloidal solutions of zinc and cadmium sulphides [8]. For an in depth introduction to the physics of fluorescence, I recommend the excellent seminars available on the web [9].

To keep a long story short, the time and colour dependency of the fluorescent light can be simply expressed in two equations implying the interaction of electrons and photons (light particles).

Time delay equation:

$$\text{Timestamp of emission of fluorescent light} = \text{Timestamp of illumination} + \text{delay of emission by excited electron.}$$

Also noted as:

$$t_{\text{emission}} = t_{\text{illumination}} + \delta t \quad (1)$$

Balance equation of energy:

$$(\text{Energy of photons} + \text{Energy of electrons} + \text{Energy of environment})_{\text{before illumination}} = (\text{Energy of photons} + \text{Energy of electrons} + \text{Energy of environment})_{\text{after fluorescence}}$$

If one chooses the zero of energy to be the energy of the environment before illumination, this balance equation can be noted as:

$$E_{\text{electrons before}} + E_{\text{illumination}} = E_{\text{electrons after}} + E_{\text{emission}} + E_{\text{environment after}} \quad (2)$$

The wealth of experimental techniques used to investigate fluorescence takes systematically advantage in one way or another of the terms of these two equations, combined with the knowledge of the spatial localization of the fluorescence interaction. For example:

- Fluorescence Lifetime Spectroscopy (FLS): timestamps of the fluorescent photons are recorded knowing the timestamp of the excitation.
- Fluorescence Correlation Spectroscopy (FCS): fluorescence intensity fluctuations are investigated with the autocorrelation function, i.e. product of the fluorescence intensity times the fluorescence intensity shifted at a later time.
- Fluorescence Lifetime Imaging Microscopy (FLIM): the lifetime of the fluorescent photons are spatially imaged for a field of fluorophores.
- Time Correlated Single Photon Counting (TCSPC): single photons are recorded at picoseconds resolution and processed in time traces or correlation calculations.

- Fluorescence Antibunching Cross Correlation: single photon detectors having a dead time of about 80 ns, the time correlation between one photon detected on one detector is correlated with photons that are detected on the other detector.
- list not exhaustive...

Core-Shell CdSe-CdS Quantum Dots

It can be said that if the possibility of controlling the type of conductivity of a semiconductor material by doping with various impurities and the idea of injecting nonequilibrium charge carriers were the seeds from which semi-conductor electronics developed, heterostructures could make it possible to solve the considerably more general problem of controlling the fundamental parameters inside the semiconductor crystals and devices: band gaps, effective masses of charge carriers and their mobilities; refractive indices; electron energy spectrum; etc.

Zhores Alferov [10]

As mentioned, the distinctive property of semi-conductors is that energy must be supplied to raise their electrons above a forbidden bandgap in order to be in the right setting to be used for different purposes like conductivity, fluorescence or signal amplification. There are two ways to engineer that semiconductor bandgap.

As a first top-down approach, one can modify the spatial confinement of the semiconductor crystal. The electronic levels in the crystal will be further quantized. This may be illustrated by Figure 2.

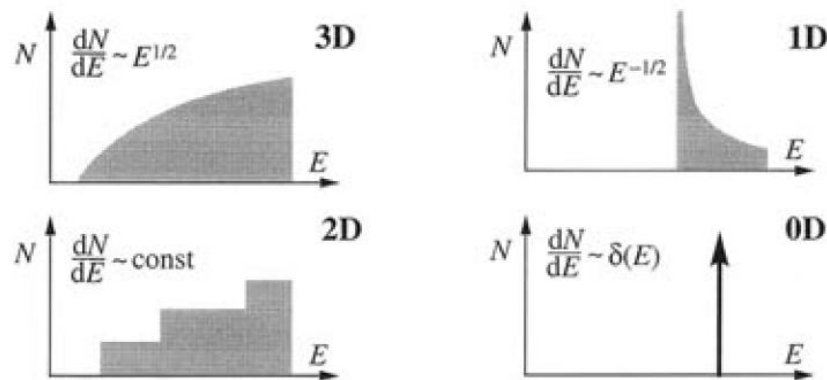
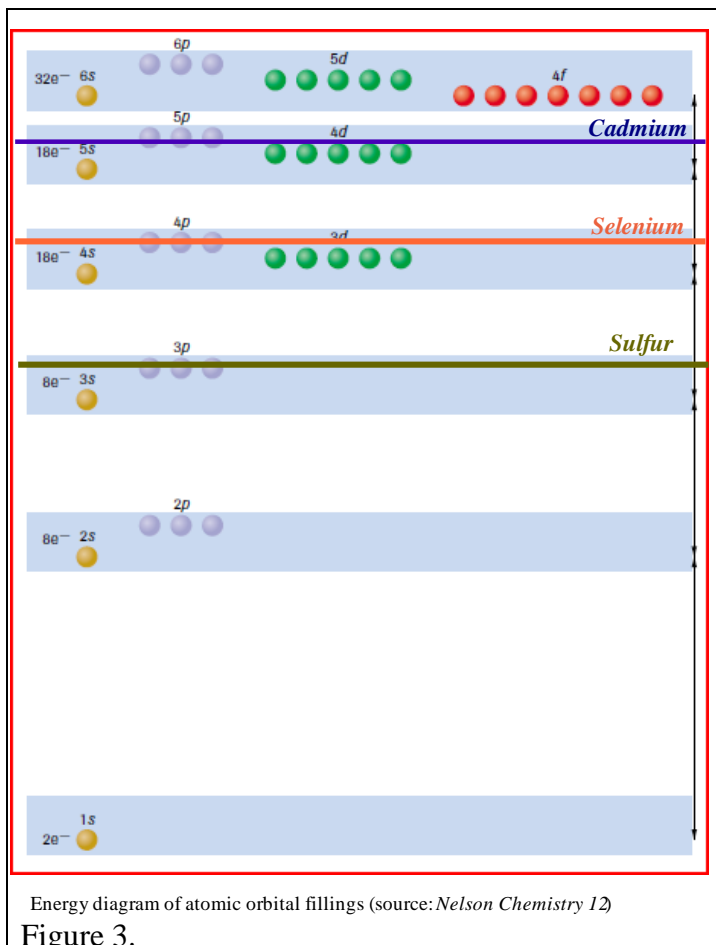


Figure 2: Density of energy states for electrons in different dimensional configurations (Source Alferov[10])

The 0-dimensional quantum dots reveal the sharpest energy spectra, comparable to those of atoms.

A complementary approach is to create heterogeneities in the crystalline structure of the material. For example, mixing cadmium atoms with selenium atoms, instead of having a homogeneous cadmium metallic crystal, creates the semiconductor bandgap. Theoretically this is solved in the effective mass approximation of the electron hole theory [11]. Ab initio local density approximation (LDA) using electron density functional theory [12, 13] can provide spatial visualization.



Energy diagram of atomic orbital fillings (source: *Nelson Chemistry 12*)

Figure 3.

The electronic configuration of cadmium is $^{48}\text{Cd} = [\text{Ar}] 3\text{d}^{10} 4\text{s}^2 4\text{p}^6 4\text{d}^{10} 5\text{s}^2$. In a cadmium crystal, the outer 5s and 4d electrons form covalent bonds or molecular orbitals which hold the atoms together. Figure 3 shows the filling of the electronic energy bands. The 5s and 4d levels are filled and their energies overlap with the 5p electronic level. Therefore, the 5s and 4d electrons are allowed to circulate across the lattice structure using the 5p conduction band vacancies. Crystalline cadmium is conductive. It is a metal.

Figure 4 tentatively shows a 1D lattice of eleven cadmium atoms on a row with its electrons represented as arrows. This figure could be extrapolated to a sphere or regular polyhedron of approximately $11*11*11 * \pi/6 \approx 700$ atoms.

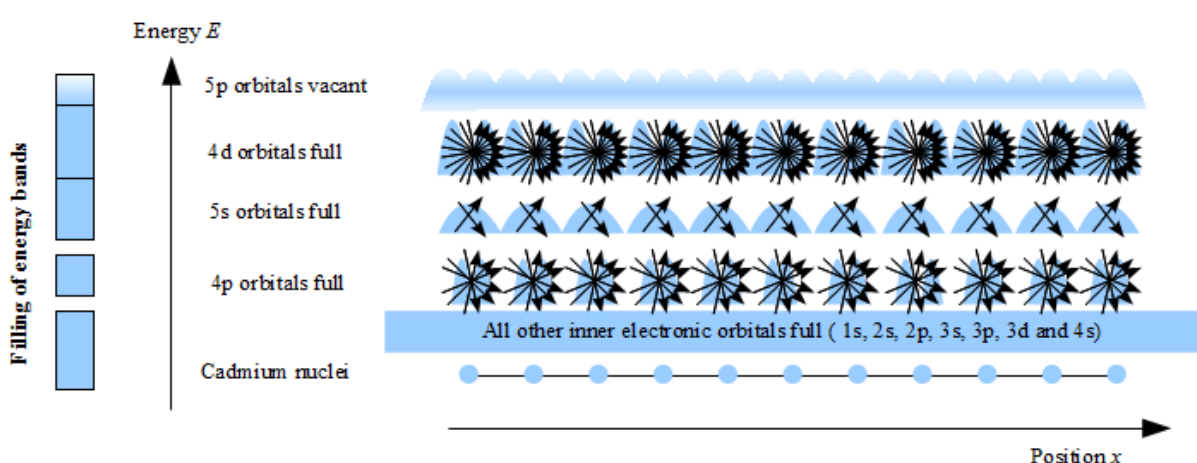


Figure 4: 1D Cadmium lattice

Suppose we bring heterogeneity in this lattice. Every second lattice point, we replace the cadmium atom by a selenium atom. The electronic configuration of selenium is $^{34}\text{Se} = [\text{Ar}] 4\text{s}^2 3\text{d}^{10} 4\text{p}^4$. In this combination, cadmium is the electropositive cation and donates its two 5s electrons to fill the 4p valence band of selenium and forming an electrovalent bond. We are thus left with a crystal, schematically represented in Figure 5 with filled Se 4p and Cd 4d levels [14]. Energy must be supplied in order to raise a 4p electron above the bandgap allowing him to circulate through the crystal. Crystalline CdSe is a semiconductor with a dominating 4p valence and 5s conduction bands. The energy of the bandgap can be determined experimentally through an absorption spectrum. For bulk CdSe at room temperature with a

wurtzite hexagonal structure, the onset of absorption is at 1.74 eV corresponding to a wavelength of 712 nm.

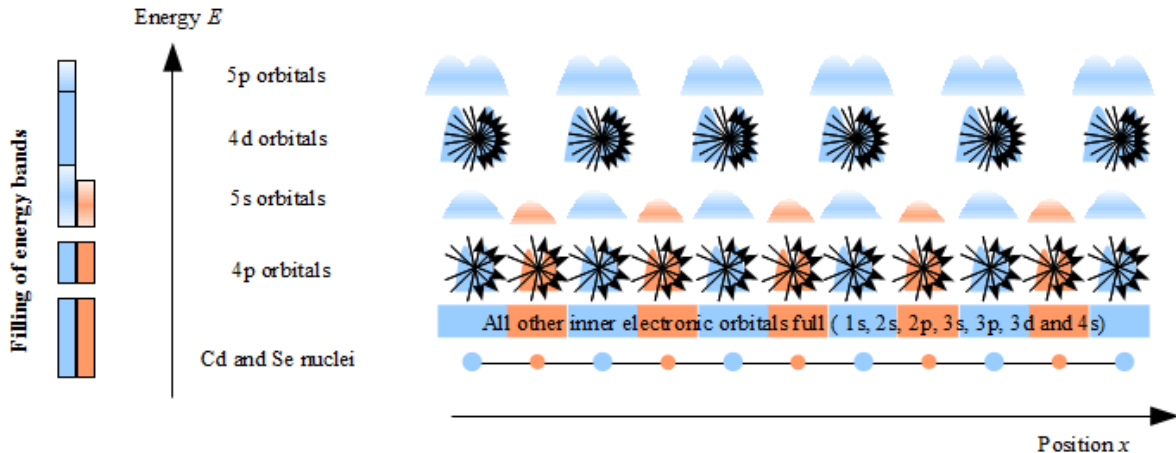


Figure 5: CdSe nanocrystal with 4p valence band and 5s conduction band

When a photon of energy higher than the bandgap energy impinges on a CdSe crystal, there is a finite probability that an electron takes up the energy and begins to circulate through the crystal, according to Equation 2, while leaving a hole at the place where it was ejected. If the electron is not ejected from the nanocrystal (ionization of the QD), the dynamics of this excited electron strongly depends on:

1. its interaction with the positively charged hole, represented by an excitonic Coulomb interaction in the effective mass approximation,
2. the boundary conditions of the nanocrystal, giving wavefunction solutions for the nanocrystal: $\exp(i \mathbf{k}_n \cdot \mathbf{r})$, see Figure 6,
3. the periodical potential of the lattice, represented by the function $u_{\mathbf{k}}(\mathbf{r}) = u_{\mathbf{k}}(\mathbf{r} + \mathbf{l})$, where \mathbf{l} is the lattice constant in the direction of the momentum vector of the electron. This potential is shaped by the local 5s electron orbitals.

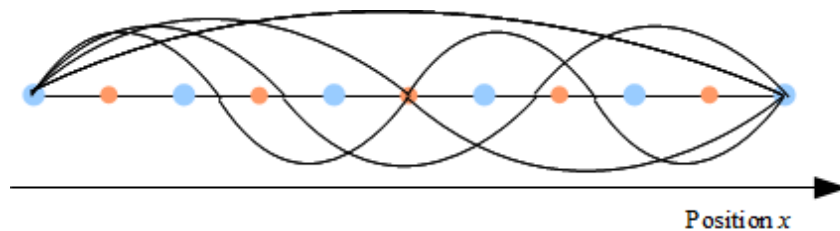


Figure 6: Wavefunction solutions for the nanocrystal for $n = 1$ to 4

The envelope functions $\exp(i \mathbf{k}_n \cdot \mathbf{r})$ and the periodical potential combine to give the Bloch functions pertaining to the quantum dot. The exact theoretical treatment of these dynamics necessitates more sophisticated models, like the $\mathbf{k.p}$ theory and Luttinger model, which can be found in review articles of the excitonic behaviour of quantum dots [11]. Figure 7 tentatively represents the concepts for the excitation of an electron by an impinging photon in the first excitonic state with lowest possible wavenumber $k_1 = 2\pi/11\ell$. The finite dimensions of this 1D quantum dot only allow 11 possible wavenumbers (i.e. 11 energies), hence the sharp quantization of energies for QDs. Furthermore, we see that the allowed energies inversely depend on the diameter $n\ell$ of the quantum dot.

For fluorescence to occur, the excited electron and hole must recombine, paying back the bandgap energy with a single photon (see equation 2). Like for atomic decay transitions, this

process has an exponential decay rate (see equation 1). For individual quantum dots and low mono-excitonic excitations, we can therefore observe antibunching [15].

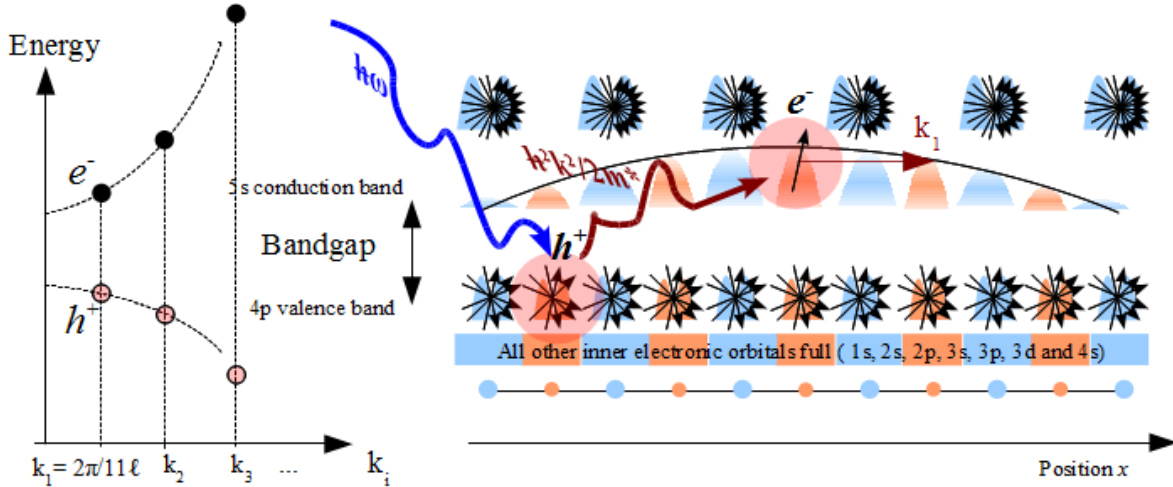


Figure 7: Excitation of an electron by a photon in a CdSe QD and formation of an exciton

So either the excited electron is ejected from the quantum dot, because of the high energy or intensity of the light beam, either the excited electron circulates through the QD with one of the allowed \mathbf{k} -vectors.

If the quantum dot is ionized, the electron and the hole will not be able to recombine, until the QD recaptures an electron (or expels the hole). The QD's fluorescence fluctuates between bright and dark time intervals. It is blinking.

In the 1S excitonic state, the excited electron has high probability to be located in the core. The remaining electrons of the valence band will spread out as much as possible, so that the vacant hole will migrate to the core. The localization of both electron and hole in the core favours a rapid non-radiative payback of energy, through electron-electron or electron-hole Auger collisions. There is only partial fluorescence, with alternating bright, so-called “grey” and dark periods.

In order to enhance the fluorescence of the quantum dot (quantum efficiency and non-blinking), we must engineer the dot in such a way as to favour radiative recombination above Auger processes and ionization. Possible solutions are:

- passivating the surface of the dot and its environment in order to prevent outflow of charge carriers,
- modifying the shape of the dot: elongated dots, planar wells, nanorods or wires,
- adding new heterostructures in the dot: a shell around the core, dopants, gradients of potential.

An exact theoretical model is still under development. Some features, like the effect of the shell on the quantum efficiency and on the fluorescence lifetime and intensities are not yet fully understood. CdS has a higher bandgap than CdSe. Growing a CdS shell around a CdSe core will therefore isolate the core from the surface, diminishing the probability for an excited electron to be trapped at surface defects. The quest for the perfect 100% quantum efficient and non-blinking QD still depends on experimental work with dots of different composition and shape. My work has been to investigate the time-resolved fluorescence for a series of core/shell CdSe/CdS quantum dots, with variable core and shell sizes.

Chemical synthesis of the quantum dots

General principles

Cores are synthesized from Cd and Se precursors according to method developed by the Cao group [16]. After that, shells are grown on the cores by reinjection of Cd and S precursors. This method was already successfully used in the LPEM group by Benoît Mahler [3].

Investigated quantum dots

By varying reinjection quantities of precursors, four types of quantum dots were synthesized by Clémentine Javaux in the LPEM chemistry lab:

- small core / small shell (PP, from French “petit coeur / petite coque”): core ø 3 nm, total ø 14 nm.
- large core / large shell (PG): core ø 3 nm, total ø 20-25 nm, not spherically shaped
- large core / small shell (GP): core ø 6 nm, total ø 17 nm.
- large core / large shell (GG): core ø 6 nm, total ø 25-30 nm.

Fluorescence Lifetime Scanning Microscopy

Principles of Fluorescence Lifetime Scanning Microscopy

We have seen that the delay of fluorescence after an excitation by an incident photon obeys a decaying exponential law, which depends on the lifetime of the excited state. Fluorescence Lifetime Scanning Microscopy is the technique that exploits this time-dependency on single molecules. This technique has undergone tremendous improvements with the development of stable short-pulsed lasers and rapid single photon avalanche detectors.

When a fluorophore in solution or in bulk is illuminated with a pulsed laser, it will emit a fluorescent signal with an exponentially decaying rate, characterized by the lifetime(s) of the excited transitions. The correlation between the instant of the pulse and the detection of the signal is investigated in Fluorescence Lifetime Spectroscopy giving characteristic decaying curves like in Figure 8.

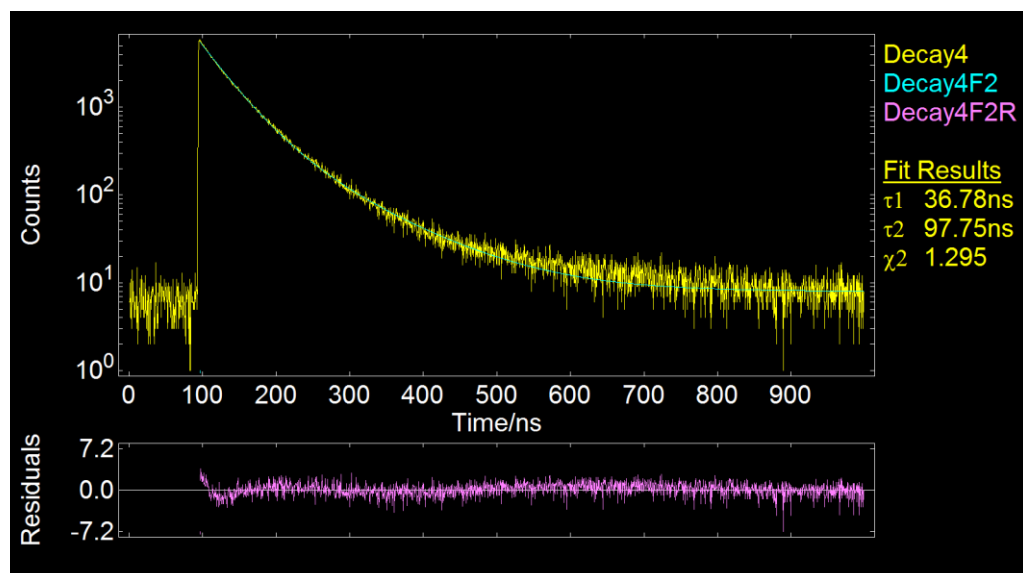


Figure 8: Fitted lifetime spectrum for a solution of CdSe/CdS Core/Shell Quantum Dots

The idea of Fluorescence Lifetime Scanning Microscopy is to direct the illuminating beam on a single nanoparticle or molecule and to record the fluorescence photon pertaining to that single nanoparticle. This can be done through confocal optics, where the excitation beam is directed through the objective onto the sample and the emission photons follow the same optical path back. Because the excitation energy is not the same as the fluorescence wavelength, they can be separated at one point of the setup with suitable filters. Figure 9 shows a scheme of the FLSM setup used during my internship. The core of this setup is the MicroTime 200 Fluorescence Microscope of PicoQuant GmbH [17].

MicroTime 200 experimental setup

Overview

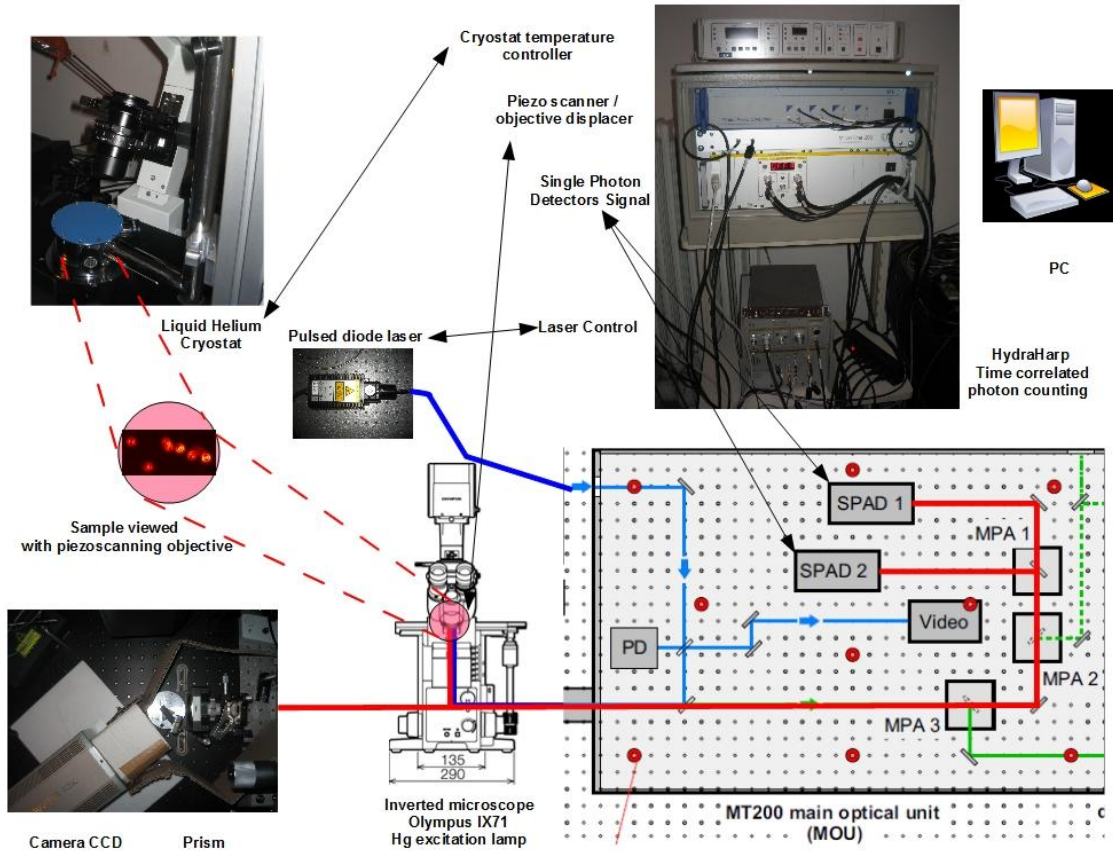


Figure 9: Scheme of the complemented MicroTime 200 experimental setup

The confocal Fluorescence Lifetime Imaging System is built around the MicroTime 200 solution. The MicroTime 200 was delivered by PicoQuant during the first week of my internship. I therefore benefited from a two-day training session by the product engineer. This solution was later on completed with some add-ons. The complete setup to date includes the following components.

MicroTime 200 components, documented in the product manual:

- Laser excitation subsystem,
- Main optical confocal unit with an inverted Olympus IX71 microscope,
- Detection subsystem,
- PC, control electronics and software.

Some add-ons complete the system:

- Mercury illuminator for the Olympus IX microscope,
- Oxford Instruments cryogenic unit,
- Single QD imaging spectrometer with CCD camera and LPEM lab specific software.

Laser excitation

The laser used for the excitation is a laser diode manufactured by PicoQuant (product LDH-D-C-405) with Peltier temperature stabilization set at 20°C. The emission wavelength is $\lambda = 402 \text{ nm}$.

The laser driver has two master frequencies 80 MHz and 1 MHz with binary dividers 1 to 32, which allows pulse repetition rates ranging from 31.25 kHz to 80 MHz. It is also possible to use laser in continuous wave. An intensity knob allows to change laser intensity, however in order to have best pulse shape, one should use laser intensity just above threshold. Intensity can also be adjusted with the help of an optical attenuator at the exit of the laser (micrometer-driven slit). The following table gives some characteristics about suitable intensity settings with respect to repetition rates. The Full Width Half Maximum is the value measured for a single pulse with the avalanche detectors without deconvolution with the impulse response function of the detectors. The minimum pulse width given by the manufacturer is 54 ps.

Repetition frequency	Master frequency and binary divider	Period	intensity knob	FWHM of convoluted peak
cw	-	-	60	-
80 MHz	80 MHz / 1	12,5 ns	37.5	180 ps
40 MHz	80 MHz / 2	25 ns	34	190 ps
20 MHz	80 MHz / 4	50 ns	34	170 ps
10 MHz	80 MHz / 8	100 ns	35	172 ps
5 MHz	80 MHz / 16	200 ns	35	168 ps
2,5 MHz	80 MHz / 32	400 ns	36	174 ps
1 MHz	1 MHz / 1	1 μs	33	171 ps
500 kHz	1 MHz / 2	2 μs	31	157 ps
250 kHz	1 MHz / 4	4 μs	29	169 ps
125 kHz	1 MHz / 8	8 μs	28	167 ps
62,5 kHz	1 MHz / 16	16 μs		
31,25 kHz	1 MHz / 32	32 μs		

The laser beam enters a single mode polarization maintaining fiber of length ~3m and its polarization is horizontal when it enters the confocal unit.

Confocal unit with Olympus IX71 microscope

The confocal unit (or Main Optical Unit – MOU – of the MicroTime 200) directs the laser beam on a diffraction limited focal spot of the sample. The useful fluorescent photons take the

return path through the microscope objective and pass a dichroic filter towards the single photon avalanche detectors. Lenses and a 30 – 150 µm pinhole collimate the fluorescent photons on the SPADs.

On its path, 10% of the laser beam is directed towards an intensity measuring photodiode.

On its back reflected path, the laser beam is also directed towards a video, which allows to control the focus in the plane of the sample.

The position of the objective of the microscope is displaced with a piezo scanner controlled by the software. The maximum useful area is 80*80µm for 150*150 pixels.

The Olympus IX71 microscope may be used for direct eye observation of the fluorescence of the quantum dots. The excitation light is provided by a mercury illuminator U-LH100HG.

Single Photon Detectors.

Two SPADs of manufacturer MPD allow detection of single photons at picoseconds time resolution. The SPADs have a dead time of 80 ns.

Acquisition card and software

MicroTime 200 is delivered with a HydraHarp acquisition card which monitors the detection.

Two detection modes are available:

- T2 mode. Only the absolute arrival times of the detected photons are recorded. No relative arrival time with respect to preceding laser pulse. This mode is used for determination of antibunching correlations.
- T3 mode. This mode synchronizes laser pulse and fluorescence photon detection via cycles: Laser pulse → detection time → dead time → laser pulse → detection time → dead time → etc.. It records each photon's timestamp relative to the preceding pulse and to the absolute start of the measurement.

MicroTime 200 is delivered with SymPhoTime software which allows triggering and processing of the spatially and time resolved fluorescence intensity traces.

Cryostat

A cryostatic Oxford Instruments sample holder allows cooling down and warming up of the observed quantum dots in a range from 4 K to 500 K.

Spectroscope

A LPEM made prism spectroscope allows recording individual quantum dot spectra.

Practical operation

The MicroTime200 regularly needs a periodical maintenance procedure aiming to prepare and realign all optical and electronics elements necessary after a break in operation inferring some thermal or mechanical drifts. Important points in this procedure are:

- Switching on the electronics: power on, laser standby set to on, detectors, piezo, HydraHarp, PC.

- Run SymPhoTime, launch the three measurement windows (video/scan, shutter control and oscilloscope).
- Mount calibration sample on microscope.
- Switch laser on, open excitation shutter → we should get some intensity on photodiode (data acquisition window > 1 a.u.), adjust laser intensity and attenuator, focus of objective and diagnostic filter wheel (OD2 or OD3) to have circular symmetric backscattered spot.
- Switch on single photon avalanche detectors. There should be dark count rates of about 30/s for SPAD1 and 150/s for SPAD2.
- For each SPAD, successively open detector shutter and variable beam-splitting route and optimize SPAD signal with time trace window using detection filter wheel (open → OD3 → mounted filter 1 for fluorescence), pinhole position, detection lens position and focus of objective.

If all optics are correctly aligned, the appropriate sample can be mounted. Choose appropriate repetition rate and run the measurements!

Measurement results

Preliminary results

The four PP, PG, GP and GG samples were synthesized two months after the beginning of my internship. Before that time and before the delivery of the cryostat, the setup was used for preliminary measurements and fluorescence lifetime imaging measurements on other samples, in order to gain practical experience of its different features.

Introductory measurements

The impulse response for the laser 402 nm pulse was measured with both SPADs active in order to get used to the response of the whole system. Figure 10 shows the time trace of the detected photons for a pulse with repetition rate 250 kHz, with a time bin smaller than the repetition period. One can read an interval of 4 μ s between 2 pulses.

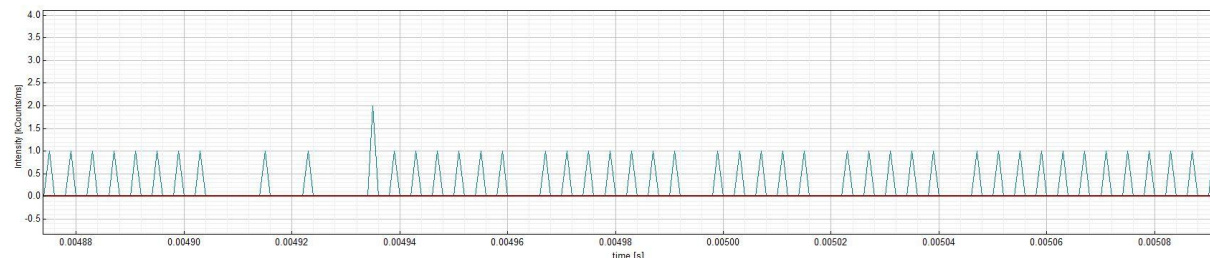


Figure 10: Time trace of 250 kHz laser pulses

Similarly, the lifetime for a single pulse is plotted, with the help of the TTTR records. Figure 11 shows the pulse convoluted with the detector response. Laser intensity is just above the lasing threshold. FWHM of the pulse is 160 ps.

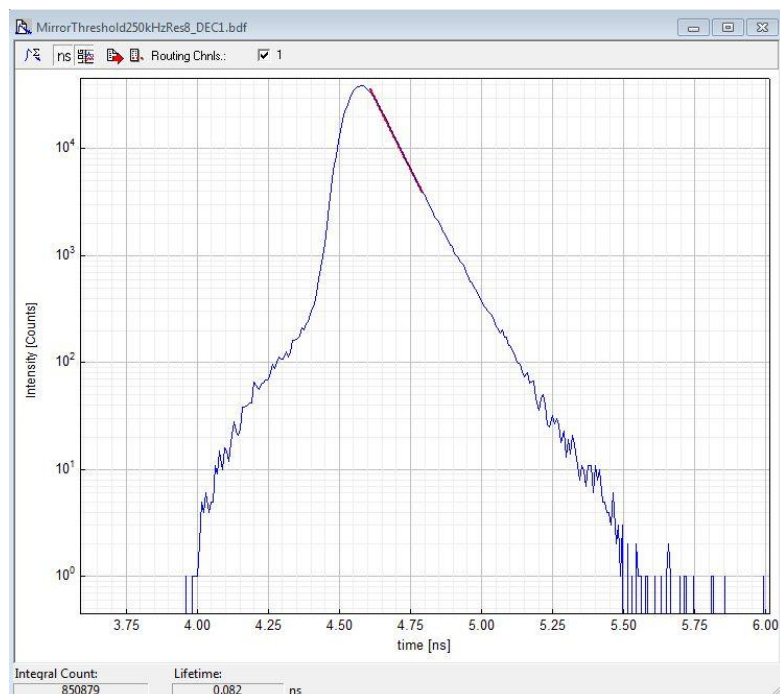


Figure 11: Laser pulse shape as detected by the SPADs

Figure 12 shows the logarithmic response during an interval of 140 ns around the pulse. This figure shows three special behaviours of the avalanche detectors:

- an “early” pulse (3 ns before the laser pulse): hypothetically caused by pre-pulse electronic activation
- afterglow at 5 – 10 ns after the laser pulse: upon detection of the laser pulse photons, SPADs tend to emit infrared photons which are back-reflected towards the other detector (path of some cm). This infrared afterglowing disappears with a shortpass or bandpass filter located before one of the SPADs. It needs to be filtered especially if one looks at antibunching of a single QD [18].
- afterpulsing at about 80 ns, which corresponds to the reactivation of the SPAD after the dead time [19].

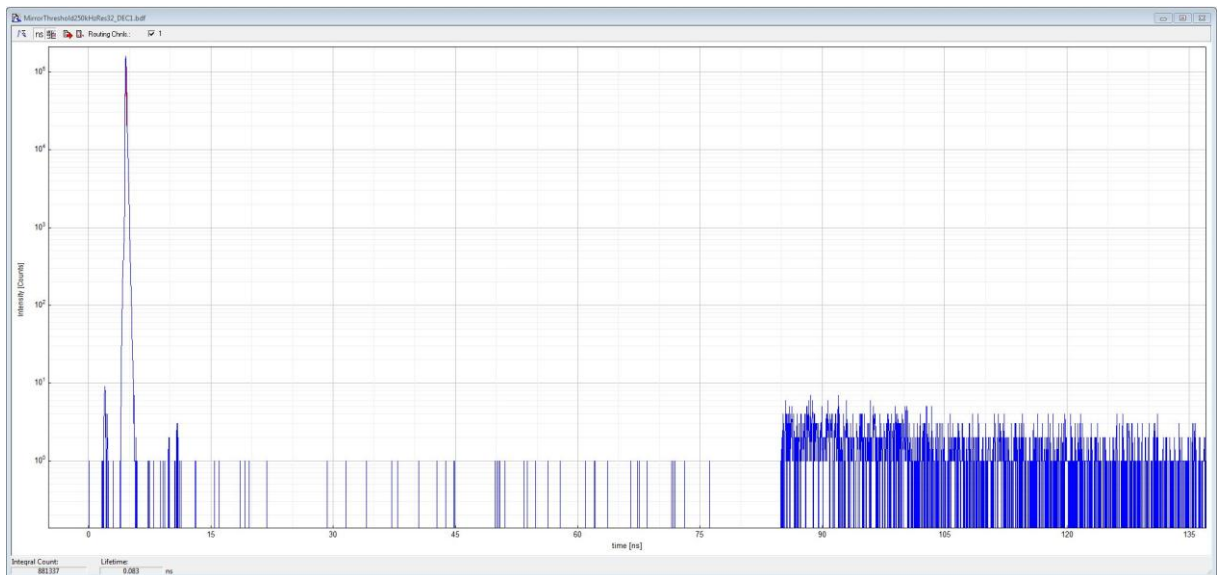


Figure 12: Time trace of mirror-reflected laser pulse

Core shell CdSe/CdS quantum dots (sample 101026)

In the first half of my internship, core-shell CdSe/CdS quantum dots were used in order to become familiar with the different SymPhoTime features. These dots were synthesized by Clémentine Javaux according to a procedure similar to that of the PG dots.

Antibunching was investigated on these QDs using a two-detector protocol. If a photon is detected by one detector, the correlation with all photons detected by the other detector during a given lag time is calculated with the second order cross-correlation function, according to the following formula:

$$g^{(2)}(\tau) = \int I_1(t)I_2(t+\tau)dt / \int I_1(t)I_2(t)dt$$

Figure 13 shows a typical diagram of the cross-correlation function, with $g^{(2)}(\tau)$ near to zero at the offset time origin.

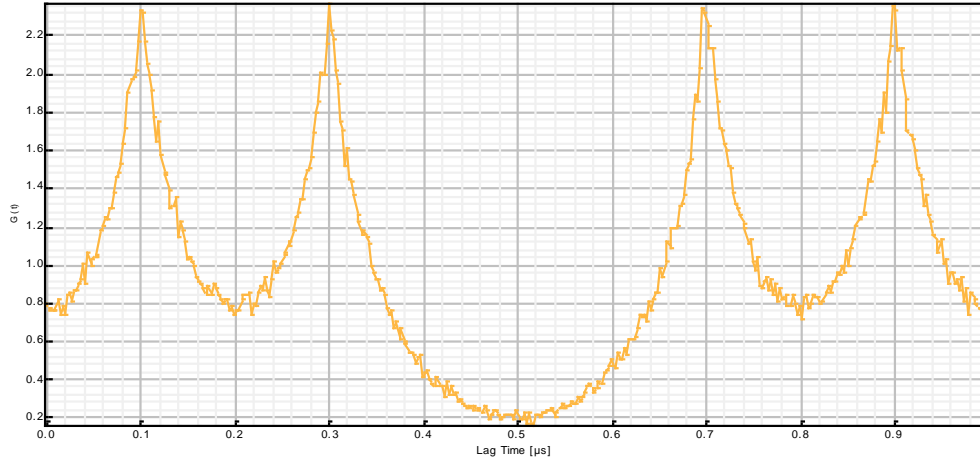


Figure 13: Antibunching effect on single QD (dot X60Y58, rep rate 5 MHz, 3 May 2010)

Figure 14 shows a typical time trace for the QDs of the sample. The intensity of the fluorescence is fluctuating between bright and low-intensity states, which are not dark states [20].

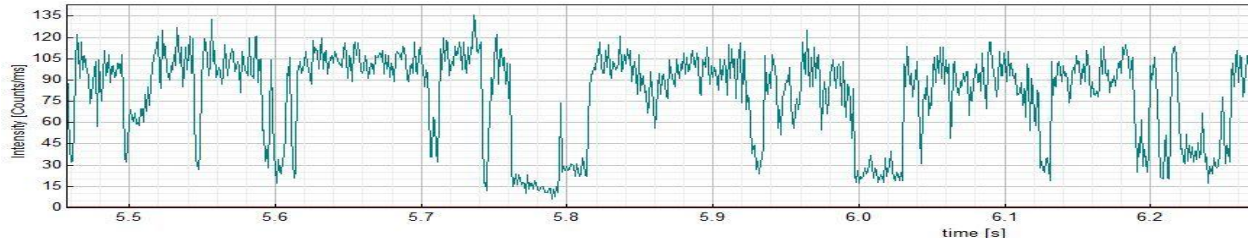


Figure 14: Time trace of quantum dot fluctuating between bright and dark states

A countrate histogram gives the proportion between bright and grey bins. Figure 15 shows four countrate histograms for the same dot illuminated with increasing laser intensity. For the lowest intensity, the dot's fluorescence intensity doesn't fluctuate. For higher excitation intensities, grey states become predominant [20].

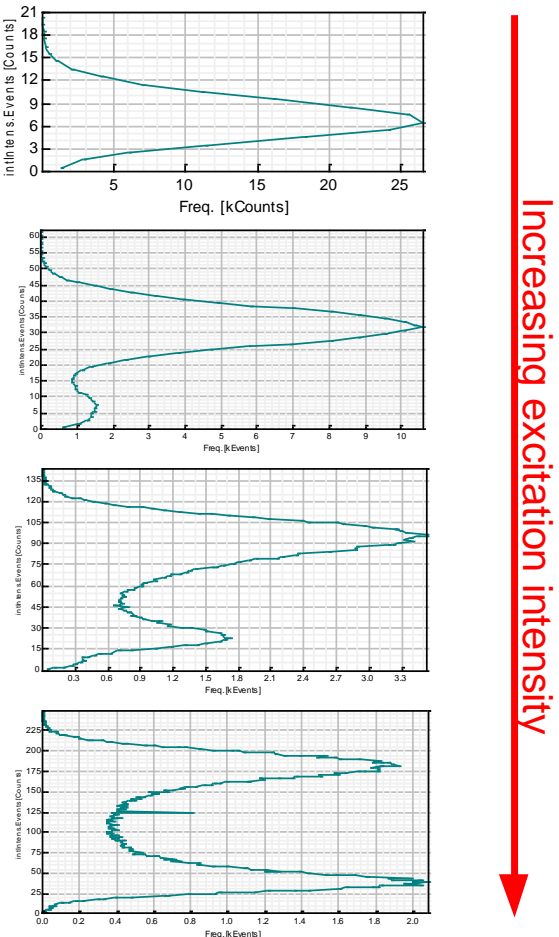
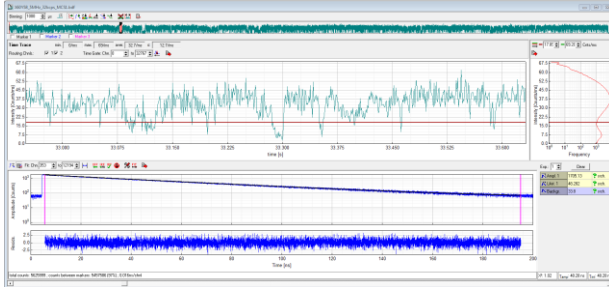


Figure 15: Counrate histograms for increasing intensities

Lifetime histograms represent the timestamp of detection for the fluorescence photons after the onset of the laser pulse. Figure 16 shows the fitted lifetime histograms for the “bright” photons and for the “grey” photons. The bright state has lifetime about 50 ns, while the grey state has two lifetimes of 27 ns and 5 ns.

Bright level: clearly monoexponential ~ 50 ns



Grey level: clearly biexponential ~ 27 ns and 5 ns

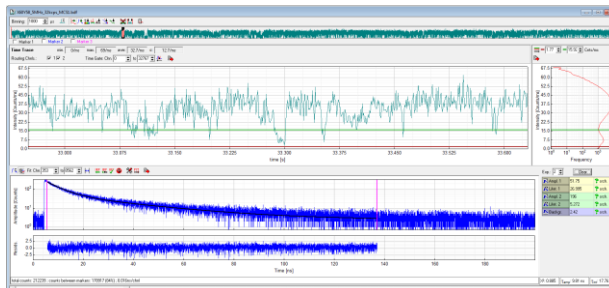


Figure 16: Lifetime histograms for the bright state and the grey state

CdSe quantum platelets

Lifetime measurements have also been performed on quantum platelets, synthesized by Mickaël Tessier [21]. Due to their different confinement condition, these platelets emit green fluorescent light. These platelets are not single photon emitters, probably due to their higher cross section. Typical antibunching measurements in the Hanbury-Twiss and Brown setup yields cross-correlation graphs similar to that of Figure 17, but without low correlation at the origin of time.

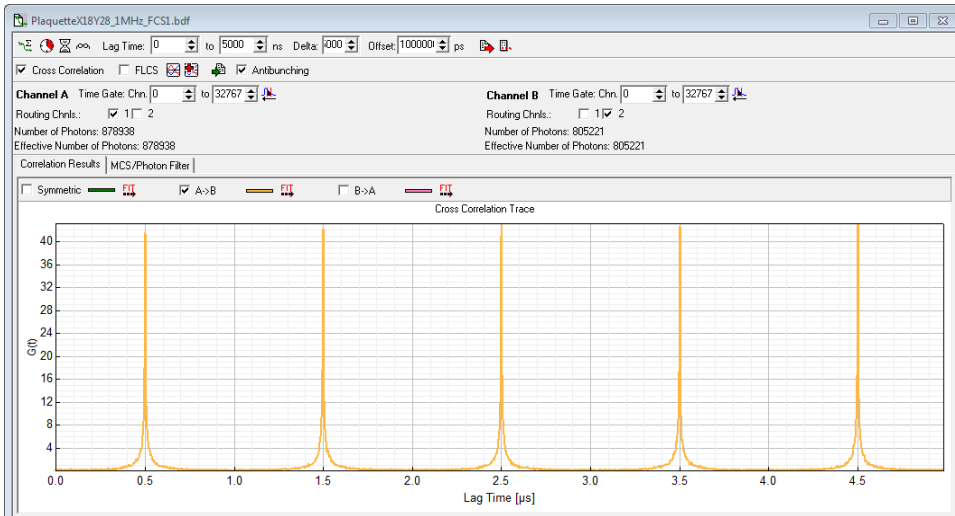


Figure 17: Cross-correlation histogram for platelets with zero-time peak at the center

Figure 18 shows the time trace and its count histogram for a platelet.

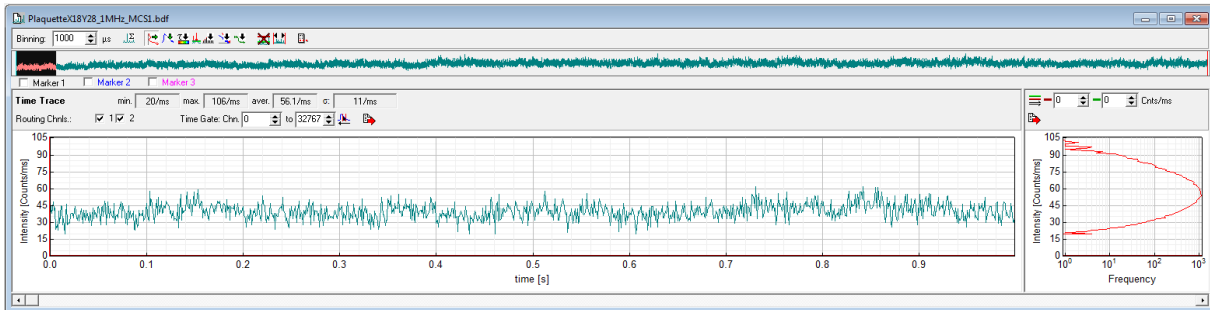


Figure 18: Fluorescence time trace for quantum platelets

Platelets have multiple lifetimes corresponding to multiple transition paths. A typical platelet's lifetime histogram is shown in Figure 19. Fitting the exponential decay yields three lifetimes: 11 ns, 3 ns and 600 ps.

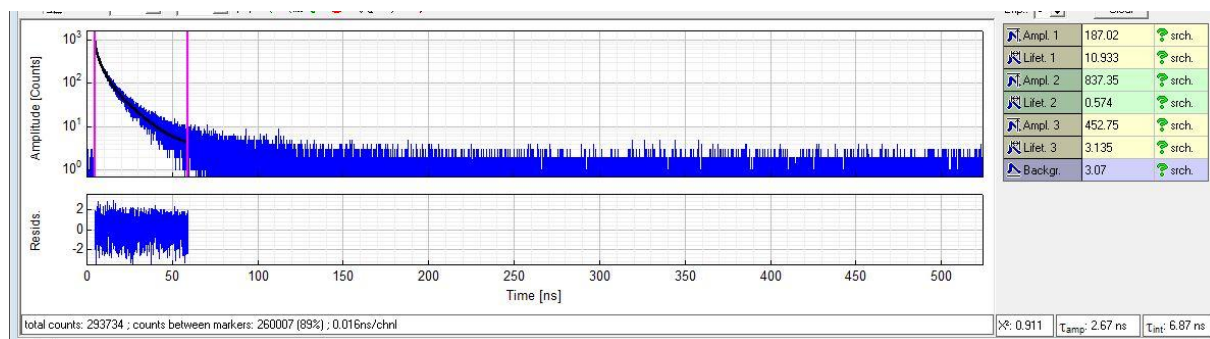
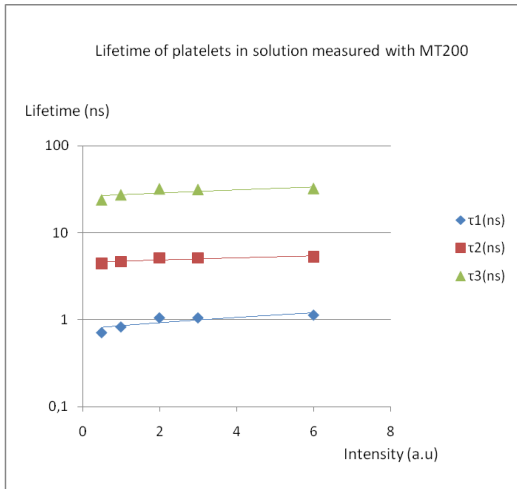


Figure 19: Lifetime platelet X37Y28, 10 May 2010

The lifetime of the platelets have also been observed with the MicroTime 200 in a milliliter solution, with different intensities. For the fit, with increasing intensities, all the lifetimes increased, see following table and graph.

Intensity (a.u.)	Amplitude1	τ_1 (ns)	Amplitude2	τ_2 (ns)	Amplitude3	τ_3 (ns)
0.5	275	0.71	331	4.42	33	23.77
1	483	0.829	537	4.68	47	27.17
2	1116	1.06	1040	5.14	84	31.88
3	1706	1.06	1488	5.15	123	31.29
6	3244	1.14	2662	5.30	210	32.12



Measurements series on the PP, PG, GP and GG quantum dots

Observation of fluorescent QDs with the eye under microscope

Prior to any lifetime measurement, the dots are observed with the eye under illumination of the mercury lamp. One can remark that the fluorescence of the thick shell dots is very stable, the large core/thick shell even being exceptionally stable and resistant to photobleaching. The fluorescence of the small shell dots is fluctuating. The PP dots photobleach after some minutes of illumination by the mercury lamp.

Emission spectra of quantum dots

The spectra of the quantum dots were measured by Clémentine Javaux on a Fluoromax-3 spectrometer from Jobin Yvon (Horiba). Figure 20 shows the emission spectra of the different dots. The maxima for each type of dot are at:

- 660 nm for GG
- 656 nm for GP
- 624 nm for PG
- 622 nm for PP

This verifies the rule that the dot's fluorescence shifts towards higher energies for smaller sizes.

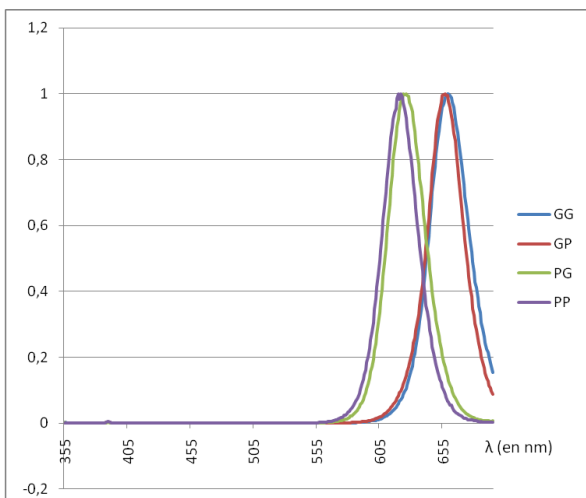


Figure 20: Emission spectra of the investigated GG, GP, PG and PP dots

Fluorescence lifetime of dots in solution

Fluorescence lifetime of the dots in solution has been measured for each sample. The results are under process.

MicroTime 200 results

Comparative results at room temperature

Caveat. The following results must be interpreted with care. Due to lack of time between the start of the measurements (May 13th 2010) and the writing of this report, measurement conditions were not always optimal. There is no guarantee for that the presented results apply to statistically representative dots of the four samples.

Antibunching

Figure 21 shows typical antibunching histograms for the core-shell dots at room temperature. Comparison is difficult because lack of a common excitation reference intensity whenever the sample is changed. One can see that there are fewer single photon emissions for large core / thick shell dots have, probably due to a higher absorption cross section and biexcitonic transition probability.

On the PP antibunching histogram one can notice little infrared afterglow sidepeaks at about -10 and +10 ns, which need to be filtered for clean histograms.

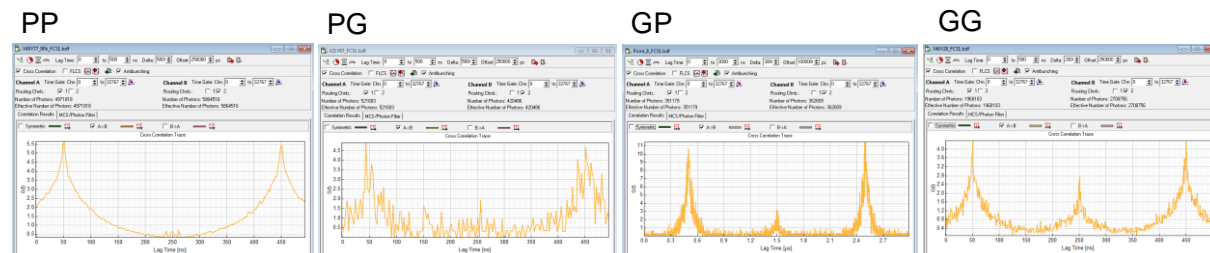


Figure 21: Antibunching histograms for different core and shell sizes

Time Traces, count rate histograms and lifetimes

Figure 22 represents the time trace, the lifetime histogram and the count rate histogram for a typical small core / small shell PP dot at room temperature and at medium intensity. The time trace shows fluctuations between a bright state and a grey state, which also appears as little low count peak in the count rate histogram. The fitted lifetime histogram yields two lifetimes: 53 ns and 5 ns.

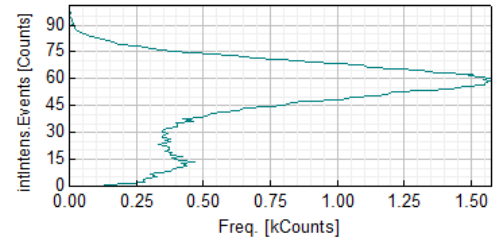
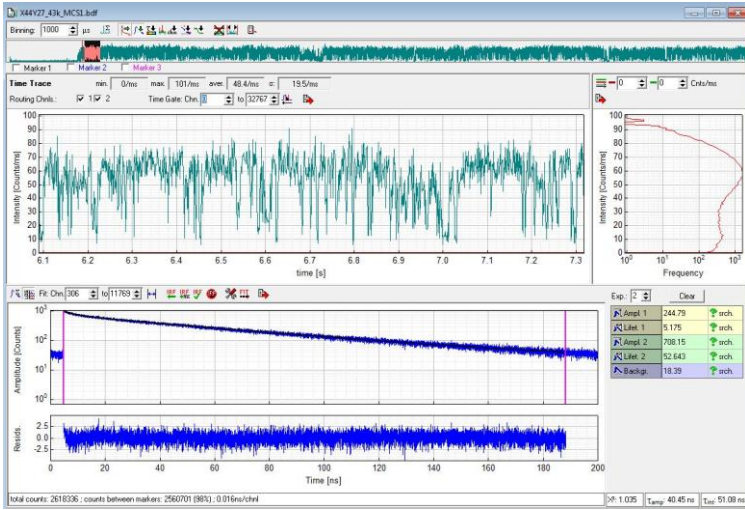


Figure 22: Measurement result for a small core / small shell quantum dot

Figure 23 represents the time trace, the lifetime histogram and the count rate histogram for a typical small core / large shell PG dot at room temperature and at medium intensity. The time trace shows a predominant grey state with “bright” bursts. Upon observation with the eye (30 ms bin time), these dots are not blinking. The fitted lifetime histogram yields two lifetimes: 35 ns and 9 ns.

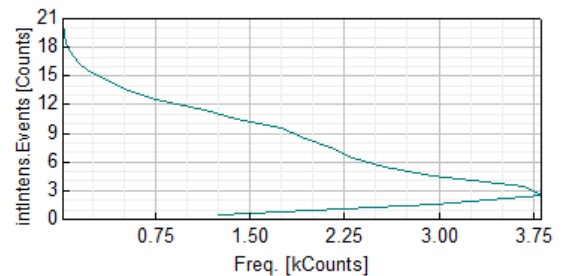
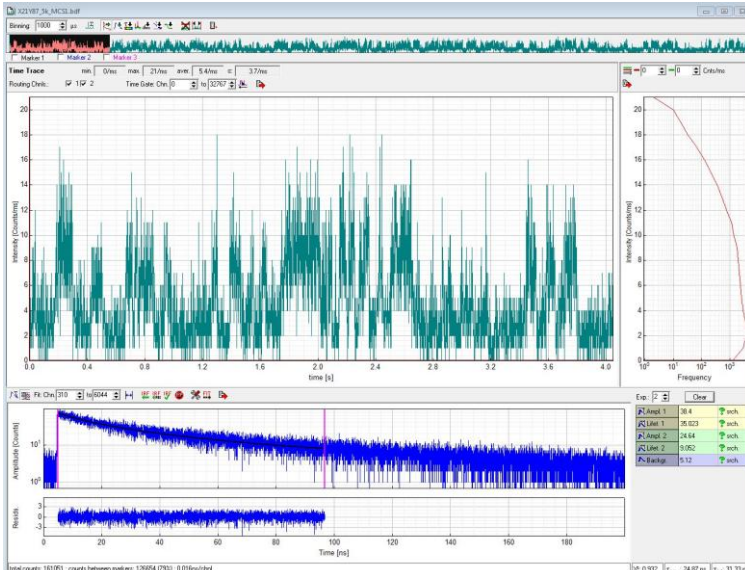


Figure 23: Measurement result for a small core / thick shell quantum dot

Figure 24 represents the time trace, the lifetime histogram and the count rate histogram for a typical large core / small shell GP dot at room temperature and at medium intensity. The time trace shows a predominant bright state with some grey periods. The fitted lifetime histogram yields three lifetimes: 53 ns, 10 ns and 1 ns.

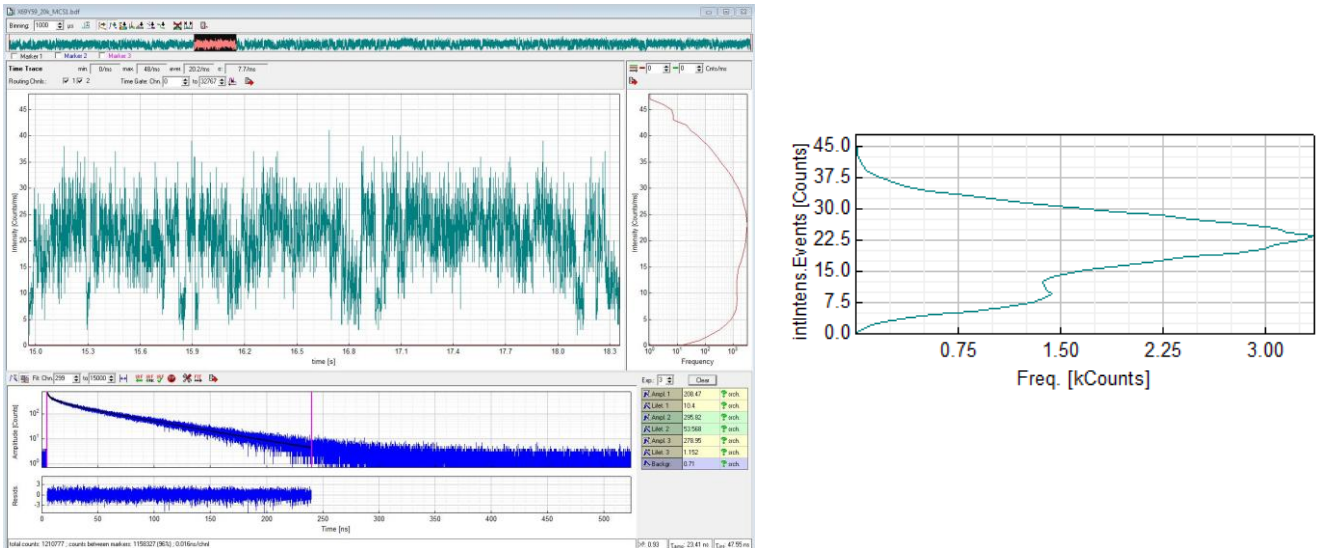


Figure 24: Measurement result for a large core / small shell quantum dot

Figure 25 represents the time trace, the lifetime histogram and the count rate histogram for a typical large core / large shell GG dot at room temperature and at medium intensity. The time trace is stable, probably a continuous “grey” state. The fitted lifetime histogram confirms this “grey” state hypothesis with two lifetimes of 11 ns and 2 ns.

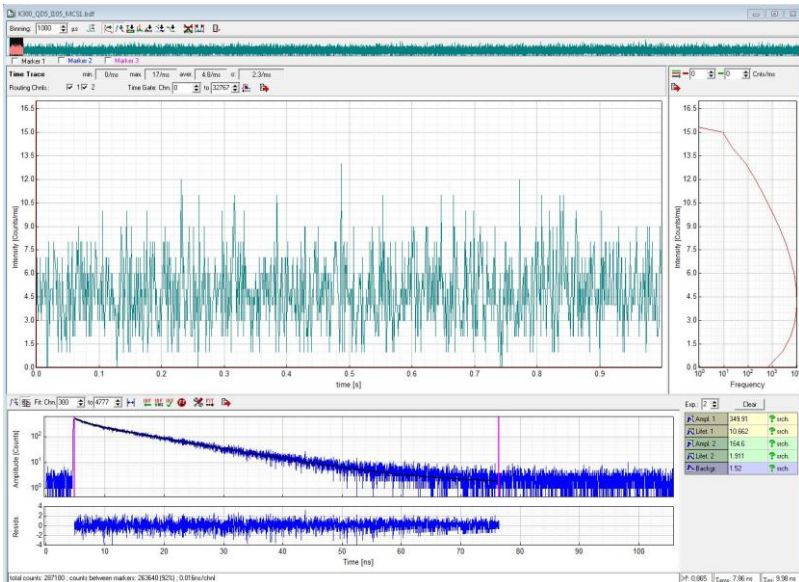


Figure 25: Measurement result for a large core / thick shell quantum dot at medium excitation intensity

Figure 26 represents the time trace, the lifetime histogram and the count rate histogram for a typical large core / large shell GG dot at room temperature and at saturation fluorescence intensity. The time trace is **exceptionally** stable. The fitted lifetime histogram yields three lifetimes: 9 ns, 1 ns and 300 ps.

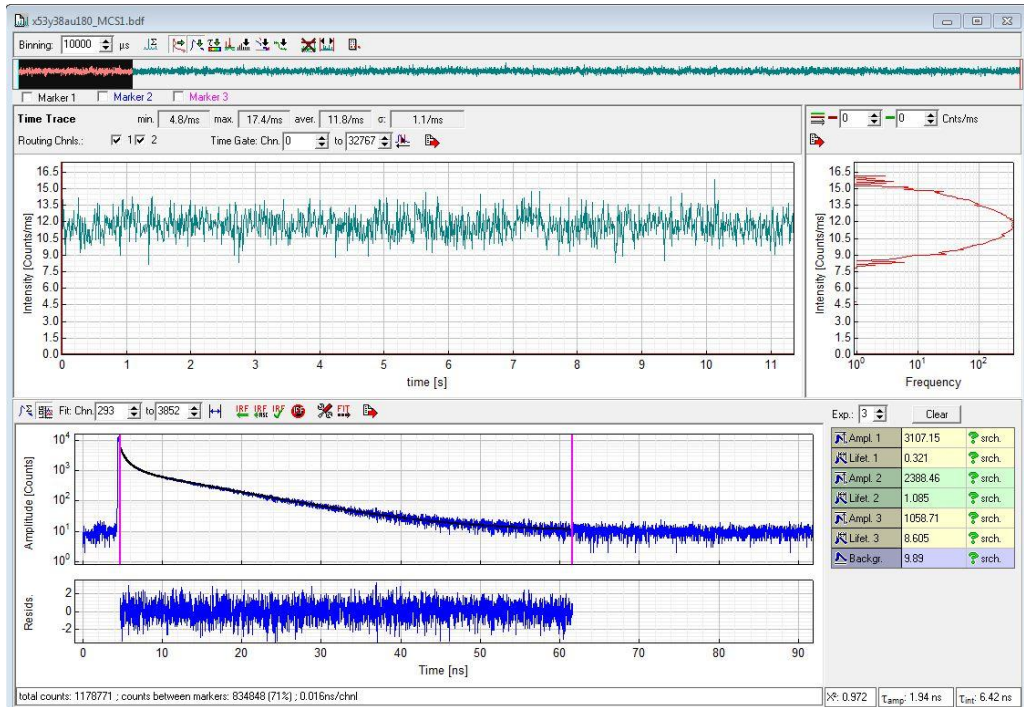


Figure 26: Measurement result for a large core / thick shell quantum dot at high excitation intensity

Results from 4 K to 300 K for GG sample

Time traces for the GG sample have been measured on 5 individual quantum dots for temperatures ranging from liquid helium to room temperature, thanks to teamwork of Benoît Dubertret, Clémentine Javaux, Benoît Mahler and me. The chosen repetition rate was 5 MHz. The time traces were recorded at 4K, 50K, 100K, 150K, 200K, 250K and 300K for three excitation intensities: low (about 2000 fluorescence photons/s), medium (1 a.u.) and high (11 a.u.). The measurement series lasted a whole day (15 hours). These measurements have not yet been processed for the other samples, because of practical difficulties. It is indeed difficult to track the fluorescence of individual quantum dots because of a variety of factors:

- Small dots bleach more rapidly than large dots. They are often lost after exposure to high intensities.
- Under vacuum conditions and room temperature, the dots lose fluorescence intensity, probably due to reactions on the surface, which trap electrons.
- There is some drift in the x-y position during the day.
- The cryogenic apparatus induces some oscillatory motions in the whole setup (UHV pump, He pump), which affects stability of fluorescence intensities reaching the detectors.

Imaging

Figure 27 shows the 43μm*43μm field of dots where time traces of 5 dots have been measured on 8 June 2010, at the start of the day (left) and at the end of the day (right). The dots had the following coordinates at the start of the day (in μm):

- QD1: x=43, y=35
- QD2: x=37, y=37
- QD3: x=50, y=33
- QD4: x=51, y=51
- QD5: x=49, y=56

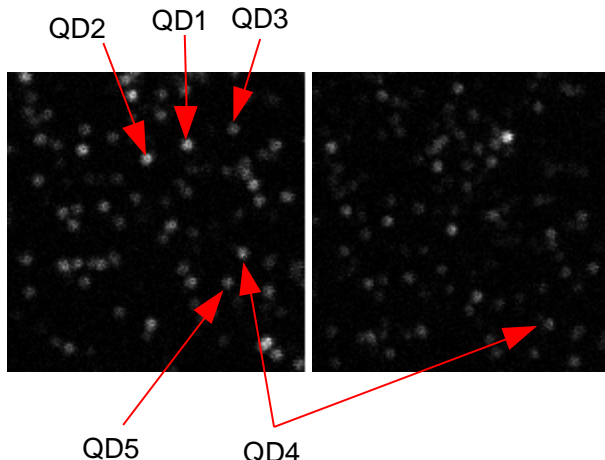


Figure 27: Field of measured quantum dots on 4K – 300K temperature range

The drift can be estimated to be about 10 μm during the whole day. One also can notice the decrease in intensity for comparable excitation intensity between 4K (start of the day) and 250K (end of the day).

Antibunching

Figure 28 shows the antibunching histogram for QD3 at 4K and medium intensity (1.05 a.u.), similar to that of Figure 21.

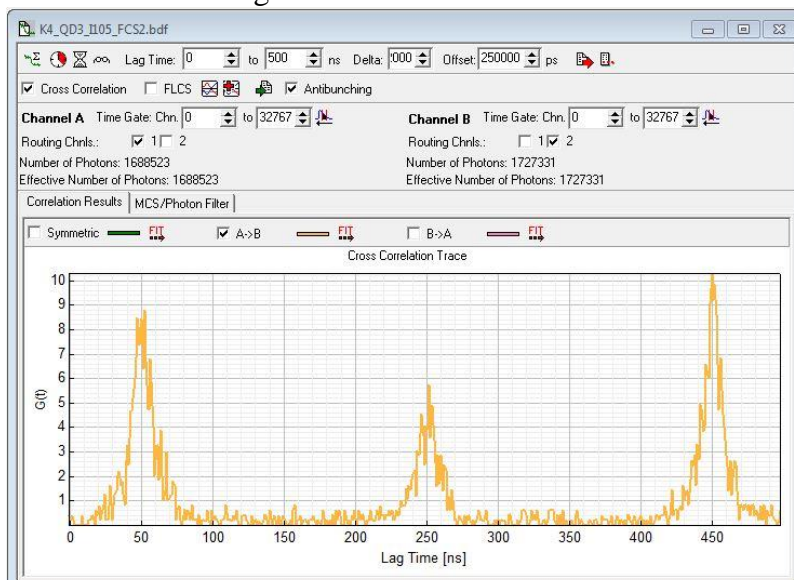


Figure 28: Antibunching diagram of QD3

Lifetimes

Like for the platelets, lifetimes of the quantum dots are intensity dependent. Moreover, there is temperature dependency, because thermal energy will affect in general the electronic transitions and more specifically the hole-electron recombinations. Figures 29 shows the lifetimes of a single quantum dot with respect to its temperature. There seems to be a counterintuitive effect of increasing lifetimes for increasing temperatures. This needs however to be further investigated. One can notice also the onset of additional lifetimes at increasing intensities, which is caused by additional paths of recombination.

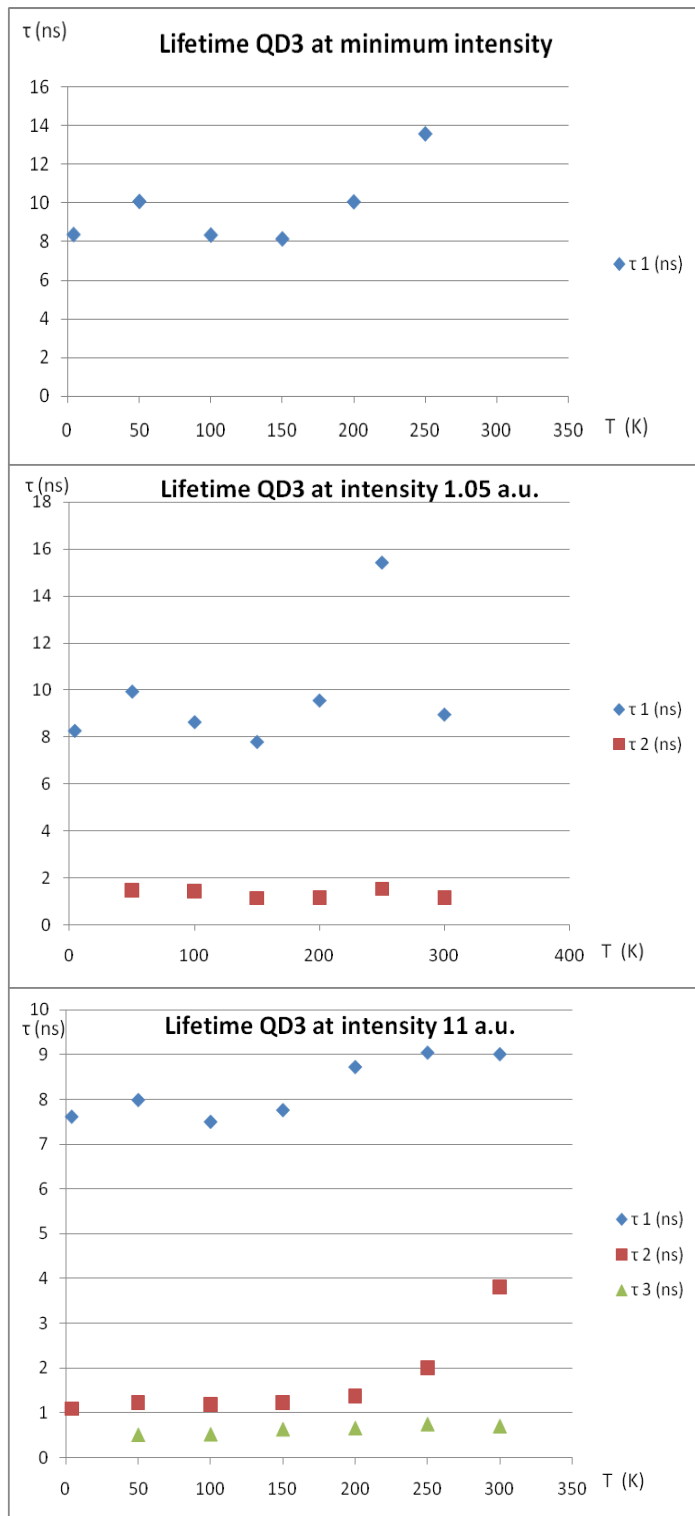


Figure 29: Lifetime dependency on temperature at various intensities. With increasing intensity, new lifetimes appear

Time traces

As an overall behavior for the five quantum dots, the fluorescence intensity diminished with increasing temperature. The time traces remained exceptionally stable, without fluorescence fluctuations other than the Gaussian spread. The results are under process.

Discussion and conclusion

The internship that I fulfilled in the LPEM group has been concentrating on the observation of time-resolved fluorescence on core-shell CdSe/CdS quantum dots with the newly acquired confocal fluorescence lifetime microscope. The most significant result is the observation of exceptional time traces of non-blinking quantum dots of a novel type: large core / thick shell, or better denoted by giant core / giant shell (core ϕ 6 nm, total ϕ 25-30 nm), emitting at 660 nm. Under observation with a transmission electron microscope, these dots are already facet shaped, polyhedral crystals. The LPEM group is the first in the world to obtain such stable fluorescence for quantum dots, even at high excitation intensities.

There remain however many questions about the precise processes that underpin its fluorescence behaviour. A surprising trend found in the measurement data is the increase of lifetime upon increase of temperature for the thick shell quantum dots. Further fluorescence lifetime investigation could provide some clues. Further comparison with the smaller dots is also needed, over temperatures ranging from 0K to 500K. Moreover, the experimental MicroTime setup can be upgraded, for example by:

- varying the excitation wavelength,
- adding polarizers that could investigate the polarization of the different lifetime photons for an individual QD,
- facilitating the processing of the measurement results by other software,
- calibrating the excitation intensity with an known reference.

On the whole, this internship was an enriching experience, where I benefited from many aspects of the ESPCI-LPEM environment:

- Qualified experts in the different subfields of the quantum dots (chemistry, optics, theory...),
- Theoretical seminars by one of the forerunners of the QD field: Dr. Alexander L. Efros,
- Relevant experimental devices for the study of QDs,
- Discussions with the LPEM staff and other graduate students.

This internship calls for a continuation, in whatever way it may be. There is still much to discover about quantum dots.

Bibliography

- [1] Ekimov, A. I.; Onushchenko, A. A., Quantum Size Effect in 3-dimensional Microscopic Semiconductor Crystals. *Jetp Letters* **1981**, 34, (6), 345-349.
- [2] Rossetti, R.; Nakahara, S.; Brus, L. E., Quantum Size Effects in the Redox Potentials, Resonance Raman-Spectra, and Electronic-Spectra of CdS Crystallites in Aqueous-Solution. *Journal of Chemical Physics* **1983**, 79, (2), 1086-1088.
- [3] Mahler, B.; Spinicelli, P.; Buil, S.; Quelin, X.; Hermier, J. P.; Dubertret, B., Towards non-blinking colloidal quantum dots. *Nature Materials* **2008**, 7, (8), 659-664.
- [4] Pauli, W., letter to Rudolph Peierls, September 29, 1931. *Volume 2 of Wolfgang Pauli, Scientific Correspondence with Bohr, Einstein, Heisenberg, a.o.*, Springer, **1979**, ISBN 3540136096, p. 94
- [5] Faraday, M., **1839**, Experimental Researches in Electricity, Vol. 1 (London: Bernard Quaritch) section 432–6
- [6] Becquerel, A. E., **1839**, *On electric effects under the influence of solar radiation*, C. R. Acad. Sci. 9 711–4
- [7] Wilson, A. H., The theory of electronic semi-conductors. *Proceedings of the Royal Society of London Series a-Containing Papers of a Mathematical and Physical Character* **1931**, 133, (822), 458-491
- [8] Sidot, Th., *Sur les propriétés de la blende hexagonale*; Note de M. Sidot, Compt. rend. 63, Paris **1866**, 188
- [9] Laboratory for Fluorescence Dynamics (Enrico Gratton Group), University of California, Irvine, Department of Biomedical Engineering, *Workshops in Advanced Fluorescence Imaging and Dynamics*: <http://www.lfd.uci.edu/workshop/> (retrieved June **2010**).
- [10] Alferov, Z. I., *Double Heterostructure Concept and its Applications in Physics, Electronics and Technology*, Nobel lecture, The Nobel Prize in Physics 2000, December 8, **2000**.
- [11] Efros, A. L.; Rosen, M.; Kuno, M.; Nirmal, M.; Norris, D. J.; Bawendi, M., Band-edge exciton in quantum dots of semiconductors with a degenerate valence band: Dark and bright exciton states. *Physical Review B* 1996, 54, (7), 4843-4856.
- [12] Wang, L. W.; Zunger, A., Pseudopotential calculations of nanoscale CdSe quantum dots. *Physical Review B* 1996, 53, (15), 9579-9582.
- [13] Hu, J. T.; Wang, L. W.; Li, L. S.; Yang, W. D.; Alivisatos, A. P., Semiempirical pseudopotential calculation of electronic states of CdSe quantum rods. *Journal of Physical Chemistry B* 2002, 106, (10), 2447-2452.
- [14] Meulenberg, R. W.; Lee, J. R. I.; Wolcott, A.; Zhang, J. Z.; Terminello, L. J.; van Buuren, T., Determination of the Exciton Binding Energy in CdSe Quantum Dots. *Acs Nano* **2009**, 3, (2), 325-330.
- [15] Michler, P.; Imamoglu, A.; Mason, M. D.; Carson, P. J.; Strouse, G. F.; Buratto, S. K., Quantum correlation among photons from a single quantum dot at room temperature. *Nature* **2000**, 406, (6799), 968-970.
- [16] Yang, Y. A.; Chen, O.; Angerhofer, A.; Cao, Y. C., Radial-position-controlled doping in CdS/ZnS core/shell nanocrystals. *Journal of the American Chemical Society* **2006**, 128, (38), 12428-12429.
- [17] *New Time-Resolved Inverted Microscope MicroTime 200*, Journal of Fluorescence, 13, 3, (2003), 287-288.
- [18] Dravins, D.; Faria, D.; Nilsson, B., Avalanche diodes as photon-counting detectors in astronomical photometry. In *Optical and Ir Telescope Instrumentation and Detectors, Pts 1 and 2*, Lye, M.; Moorwood, A. F. M., Eds. 2000; Vol. 4008, pp 298-307.

- [19] Fore, S.; Laurence, T. A.; Hollars, C. W.; Huser, T., Counting constituents in molecular complexes by fluorescence photon antibunching. *Ieee Journal of Selected Topics in Quantum Electronics* **2007**, 13, (4), 996-1005.
- [20] Spinicelli, P.; Buil, S.; Quelin, X.; Mahler, B.; Dubertret, B.; Hermier, J. P., Bright and Grey States in CdSe-CdS Nanocrystals Exhibiting Strongly Reduced Blinking. *Physical Review Letters* **2009**, 102, (13).
- [21] Tessier, Mickaël. *Rapport de stage, Master Sciences des matériaux et des nano-objets. Synthèse et caractérisation de puits quantiques colloïdaux.* 15 février – 15 juin 2010

Glossary

CCD : Charge-Coupled Device

ESPCI : Ecole Supérieure de Physique et de Chimie Industrielles de la Ville de Paris

FCS : Fluorescence Correlation Spectroscopy.

FLIM : Fluorescence Lifetime Imaging

FLSM : Fluorescence Lifetime Scanning Microscopy (or Microscope)

FWHM : Full Width Half Maximum

GG : Gros Coeur / Grosse Coque (Large Core / Thick Shell)

GP : Gros Coeur / Petite Coque (Large Core / Small Shell)

LPEM : Laboratoire de Physique et d'Etude des Matériaux, previously Laboratoire Photons et Matière

MOU : Main optical unit

OD : Optical Density

PG : Petit Coeur / Grosse Coque (Small Core / Thick Shell)

PP : Petit Coeur / Petite Coque (Small Core / Small Shell)

QD : Quantum Dots

QP : Quantum Platelets

QW : Quantum Wells

SPAD : Single Photon Avalanche Detector

SYNC : Synchronous signal driving the time correlated detection of fluorescence photons after a laser pulse

TCSPC : Time Correlated Single Photon Counting

TTTR : Time Tagged Time Resolved file format recording each detected photon with its absolute and relative time stamp.

Appendix

One appendix: Bibliographical study for fluorescence fluctuations of CdSe quantum dots.